Effect of surface type on structural and optical properties of Ag nanoparticles formed by dewetting

Irem Tanyeli,[1,2,4] Hisham Nasser,[1,3] Firat Es,[1,3] Alpan Bek,[1,2,*] and Raşit Turan[1,2]

[1]*Center for Solar Energy Research and Applications, Middle East Technical University, Dumlupinar Blvd. 1, Cankaya, Ankara 06800, Turkey*
[2]*Department of Physics, Middle East Technical University, Dumlupinar Blvd. 1, Cankaya, Ankara 06800, Turkey*
[3]*Micro and Nanotechnology Program of Graduate School of Natural and Applied Sciences, Middle East Technical University, Dumlupinar Blvd. 1, Cankaya, Ankara 06800, Turkey*
[4]*Currently with the Dutch Institute for Fundamental Energy Research, Trilateral Euregio Cluster, 3430 BE Nieuwegein, The Netherlands*
[*]*bek@metu.edu.tr*

Abstract: Integration of an array of Ag nanoparticles in solar cells is expected to increase light trapping through field enhancement and plasmonic scattering. Requirement of Ag nanoparticle decoration of cell surfaces or interfaces at the macro-scale, calls for a self-organized fabrication method such as thermal dewetting. Optical properties of a 2D array of Ag nanoparticles are known to be very sensitive to their shape and size. We show that these parameters depend on the type of the substrate used. We observe that the average nanoparticle size decreases with increasing substrate thermal conductivity and nanoparticle size distribution broadens with increasing surface roughness.

OCIS codes: (240.6680) Surface plasmons; (240.3695) Linear and nonlinear light scattering from surfaces; (290.5850) Scattering, particles; (310.6628) Subwavelength structures, nanostructures; (350.6050) Solar energy.

References and links

1. K. R. Catchpole and A. Polman, "Plasmonic solar cells," Opt. Express **16**(26), 21793–21800 (2008).
2. V. E. Ferry, J. N. Munday, and H. A. Atwater, "Design considerations for plasmonic photovoltaics," Adv. Mater. **22**(43), 4794–4808 (2010).
3. M. D. Yang, Y. K. Liu, J. L. Shen, C. H. Wu, C. A. Lin, W. H. Chang, H. H. Wang, H. I. Yeh, W. H. Chan, and W. J. Parak, "Improvement of conversion efficiency for multi-junction solar cells by incorporation of Au nanoclusters," Opt. Express **16**(20), 15754–15758 (2008).
4. F. J. Beck, A. Polman, and K. R. Catchpole, "Tunable light trapping for solar cells using localized surface plasmons," J. Appl. Phys. **105**(11), 114310 (2009).
5. S. Vedraine, P. Torchio, D. Duché, F. Flory, J. J. Simon, J. Le Rouzo, and L. Escoubas, "Intrinsic absorption of plasmonic structures for organic solar cells," Sol. Energy Mater. Sol. Cells **95**, S57–S64 (2011).
6. H. R. Stuart and D. G. Hall, "Island size effects in nanoparticle-enhanced photodetectors," Appl. Phys. Lett. **73**(26), 3815–3817 (1998).
7. R. Santbergen, T. L. Temple, R. Liang, A. H. M. Smets, R. A. C. M. M. van Swaaij, and M. Zeman, "Application of plasmonic silver island films in thin-film silicon solar cells," J. Opt. **14**(2), 024010 (2012).
8. U. Güler and R. Turan, "Effect of particle properties and light polarization on the plasmonic resonances in metallic nanoparticles," Opt. Express **18**(16), 17322–17338 (2010).
9. C. Hägglund, M. Zäch, and B. Kasemo, "Enhanced charge carrier generation in dye sensitized solar cells by nanoparticle plasmons," Appl. Phys. Lett. **92**(1), 013113 (2008).
10. F. J. Beck, S. Mokkapati, and K. R. Catchpole, "Light trapping with plasmonic particles: beyond the dipole model," Opt. Express **19**(25), 25230–25241 (2011).
11. S. Mokkapati, F. J. Beck, A. Polman, and K. R. Catchpole, "Designing periodic arrays of metal nanoparticles for light-trapping applications in solar cells," Appl. Phys. Lett. **95**(5), 053115 (2009).
12. K. R. Catchpole and A. Polman, "Design principles for particle plasmon enhanced solar cells," Appl. Phys. Lett. **93**(19), 191113 (2008).
13. H. Tan, R. Santbergen, A. H. M. Smets, and M. Zeman, "Plasmonic light trapping in thin-film silicon solar cells with improved self-assembled silver nanoparticles," Nano Lett. **12**(8), 4070–4076 (2012).

#188620 - $15.00 USD Received 10 Apr 2013; revised 1 Jul 2013; accepted 3 Jul 2013; published 31 Jul 2013

14. F. J. Beck, S. Mokkapati, A. Polman, and K. R. Catchpole, "Asymmetry in photocurrent enhancement by plasmonic nanoparticle arrays located on the front or on the rear of solar cells," Appl. Phys. Lett. **96**(3), 033113 (2010).
15. O. Gülseren, Department of Physics, Bilkent University, 06880 Ankara, Turkey, (personal communication, 2012).
16. F. Célarié, M. Ciccotti, and C. Marlière, "Stress-enhanced ion diffusion at the vicinity of a crack tip as evidenced by atomic force microscopy in silicate glasses", *http://arxiv.org/abs/cond-mat/0512567*.
17. P. Chaudhari, "Hillock growth in thin films," J. Appl. Phys. **45**(10), 4339–4346 (1974).
18. C. Y. Chang and R. W. Vook, "Thermally induced hillock formation in Al-Cu films," J. Mater. Res. **4**(05), 1172–1181 (1989).
19. E. Iwamura, T. Ohnishi, and K. Yoshikawa, "A study of hillock formation on Al-Ta alloy films for interconnections of TFT-LCDs," Thin Solid Films **270**(1-2), 450–455 (1995).
20. Y. Okada and Y. Tokumaru, "Precise determination of lattice parameter and thermal expansion coefficient of silicon between 300 and 1500 K," J. Appl. Phys. **56**(2), 314–320 (1984).
21. H. R. Shanks, P. D. Maycock, P. H. Sidles, and G. C. Danielson, "Thermal conductivity of silicon from 300 to 1400°K," Phys. Rev. **130**(5), 1743–1748 (1963).
22. C. J. Glassbrenner and G. A. Slack, "Thermal conductivity of silicon and germanium from 3°K to the melting point," Phys. Rev. **134**(4A), A1058–A1069 (1964).
23. C. M. Fang, G. A. de Wijs, H. T. Hintzen, and G. de With, "Phonon spectrum and intrinsic thermal properties of cubic Si_3N_4 from first-principles calculations," J. Appl. Phys. **93**(9), 5175–5180 (2003).
24. J. F. Shackelford and W. Alexander, *CRC Materials Science and Engineering Handbook* (CRC Press, 2000).
25. S. M. Sze, *Physics of Semiconductor Devices* (John Wiley and Sons Inc., 1981).
26. N. Oka, K. Kimura, T. Yagi, N. Taketoshi, T. Baba, and Y. Shigesato, "Thermophysical and electrical properties of Al-doped ZnO films," J. Appl. Phys. **111**(9), 093701 (2012).
27. C. F. Bohren and D. R. Huffman, *Absorption and Scattering of Light by Small Particles* (Wiley-VCH, 1983).

1. Introduction

Localized surface plasmon oscillations induced in metal particles by an electromagnetic field is expected to be useful in light trapping applications in solar cells [1]. This is based on the prediction of an improvement in the energy conversion efficiency through either near field enhancement effect in the close vicinity of the particles, or through an improved effective scattering into the active area of the solar cell [2]. In the last decade, many theoretical and design studies on different metal nanoparticle-solar cell systems have predicted significant increase in solar cell efficiency [3–5]. These predictions are generally based on well-defined, regularly distributed nanoparticle systems with ideal optical properties. In reality, most of the experimental studies deal with randomly distributed nanoparticles that are prepared from thin metal films by thermally induced self-organized dewetting of the underlying substrate surface [6,7]. Even in the case of size wise mono-disperse and periodic nanostructure systems fabricated by sophisticated techniques such as e-beam lithography [8,9], a small deviation from the intended structure shape or size causes significant changes in the resultant optical spectrum of the system [10–12]. It was indeed shown that the shape, size, and distribution of metal nanoparticles should be carefully controlled in order to create a positive impact on solar cell performance [2,13,14]. Any parasitic absorption by the nanoparticles might lead to a loss in the supply of the light into the active cell area. As a result, the experimental studies have not been able to undoubtedly demonstrate the expected breakthrough with respect to the state-of-the art solar cells with light trapping structure based on traditional surface texturing [7].

Ag nanoparticles (AgNPs) are of particular interest in solar cell research for their preferable resonance behaviour in the visible spectrum. The AgNPs attract more attention with respect to Au nanoparticles (AuNPs) because it is calculated that an effective maximum path length enhancement in the presence of absorption for AgNPs is about twice as high as the path length enhancement for AuNPs [12]. Thus, it is preferable to use AgNPs and, by choice of the dielectric environment, the resonance can shift to the desired wavelength range. AgNPs can be prepared either by high resolution lithography or by techniques which are relatively more appropriate for mass production such as dewetting [6] and self-assembly methods [7]. Recently, several studies have reported on the different aspects of AgNP-solar cell systems that are fabricated by both techniques [5,7,13]. However yet, the effect of the substrate on the formation kinetics of the nanoparticles and the optical properties of the combined system are not studied intensively.

#188620 - $15.00 USD Received 10 Apr 2013; revised 1 Jul 2013; accepted 3 Jul 2013; published 31 Jul 2013

In this article, we report on dewetting based fabrication and optical responses of AgNPs on 5 different solar cell technology relevant material surfaces which are widely used, namely Si, SiO_2, Si_3N_4, InSnO (ITO), and Al doped ZnO (AZO). We believe the results of such a comparative study on these various solar cell technology relevant substrate surfaces will be highly beneficial and may help paving the way to discovery of the most important factors for controlling the average nanoparticle size, and the breadth of the size distribution. These material systems are of interest as they are used in the front and back surfaces of c-Si and thin film solar cells or as intermediate layers for various functionalities.

2. Experimental methods

Due to rapid degradation of AgNPs in ambient conditions the sample preparation, fabrication and measurements were performed in the same day for all sets while keeping them in an N_2 desiccator storage chamber during the interval periods between various measurements.

2.1 Fabrication procedure

For dewetting based formation of AgNPs, we first thermally evaporated 12 nm Ag film on 5 different substrate surfaces. These substrates were (I) single crystalline Si wafer, (II) ~60 nm thermally grown SiO_2 on Si wafer, (III) 75 nm PECVD deposited Si_3N_4 on Si wafer, sputtering deposited (IV) 15-30 nm ITO and (V) 300 nm AZO on glass. The Si wafer was dipped in HF solution shortly before Ag evaporation for removal of native oxide. 5 sets of each ~4 cm^2 samples were prepared from each substrate. One set from each substrate type was kept as grown with the Ag film at room temperature, and one set of each substrate type was then identically annealed under 150 sccm N_2 flow at each temperature of 200 °C, 300 °C, 400 °C, and 500 °C for 60 minutes.

2.2 SEM and AFM imaging and analysis

A total of 20 annealed samples were imaged by a field emission SEM (FEI). Surface roughness was measured by an AFM (Veeco Nanoscope5) in tapping mode. The images were analysed by the image analysis software (Gwyddion, http://gwyddion.net/) to obtain size distributions of AgNPs on each sample. The nanoparticles were marked by threshold using grain analysis tool of the software. First, a mask was created using the marked grains; second, the spikes and incomplete grains at the image border were rejected from the mask. The average sizes of nanoparticles were derived either directly from the statistics toolbox of the software or from the equivalent radius of a disk of equivalent area to that of each marked grain.

2.3 The optical properties

Figure 1 shows a sketch of the optical reflection measurement setup used in this report.

#188620 - $15.00 USD Received 10 Apr 2013; revised 1 Jul 2013; accepted 3 Jul 2013; published 31 Jul 2013

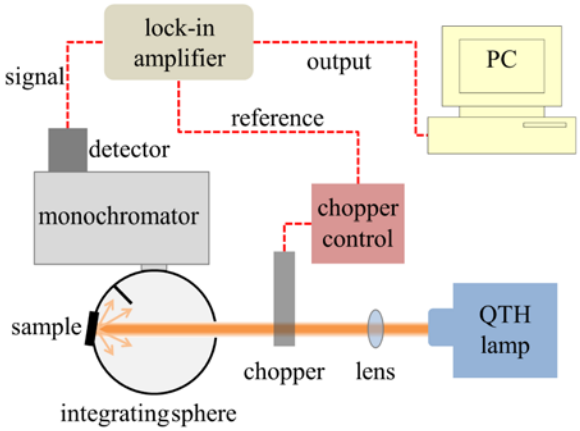

Fig. 1. The reflection measurement system consists of a QTH lamp, a chopper and its controller, an integrating sphere, a monochromator, a detector, a lock-in amplifier and a PC. The sample is mounted with a 4° offset angle to ensure measurement of total reflection.

The optical responses of the AgNP decorated samples were obtained by measuring the total reflection using an integrating sphere (Newport 70679NS) coupled to a monochromator (Newport Cornerstone 260). The light from a quartz halogen lamp (QTH, Oriel 60000 Series) was collimated and directed onto the surface of the sample of interest which was mounted on a holder with a 4° angle with the normal of the incoming light. This configuration provided for multiple reflections in the integrating sphere. The diffused light was fed into the entrance slit of the monochromator and reached a Si photodiode detector (Newport 70356). The measurements were taken in the range of 300 - 1100 nm. The raw data were dark count subtracted and normalized to the reflection signal from a near Lambertian white spectral calibration disk (Newport 70496).

3. Results

3.1 Role of the annealing temperature

Figures 2 and 3 display, in columns from left to right, SEM images, size distribution histograms, and the total optical reflection spectra of AgNP decorated surfaces of 5 different substrate types which are fabricated by thermal dewetting of a 12 nm Ag film after annealing for 1 h at 300 °C and 500 °C, respectively. Similar data were obtained for annealing temperatures of 200 °C and 400 °C which are not shown here due to space limitations. The red scale bar on SEM images corresponds to a distance of 1 μm on each SEM image. Magnitude of the substrate projected areas of regularly and irregularly shaped AgNPs are represented with the radius of an equivalent circular disc having identical area for each AgNP. The size distribution analyses were made on SEM images of 36 μm^2 large square regions on each sample. For a clear view of AgNPs, the SEM images displayed on the leftmost column in both Figs. 2 and 3 show smaller yet representative regions of the original square on which the statistics were performed.

The y-axes of the size histograms represent the frequency of AgNPs in percentage corresponding to equivalent disc radii as given in the x-axes. The effect of annealing temperature and the substrate are clearly seen from the differences in all aspects of the resultant data. The shape of the AgNPs appears to be more spherical and homogenous for Si substrate than the AgNPs on other substrates for both annealing temperatures. The nanoparticles are also more homogenously distributed in size and can be fit by a Gaussian curve with a very high correlation coefficient of $R = 0.99$. For Si_3N_4, both the shape and the size distribution are more inhomogeneous with more than twice the FWHM breadth compared to that for Si substrate. We see that the AgNPs have less regular shape and, the size distribution cannot be perfectly described by a single Gaussian curve. Similarly, we see two

#188620 - $15.00 USD Received 10 Apr 2013; revised 1 Jul 2013; accepted 3 Jul 2013; published 31 Jul 2013

groups of AgNPs on the SiO_2 sample surface annealed at 300 °C, one peaked at a radius of around 13 nm, and the other at around 57 nm. As surface diffusivity of smaller particles might be expected to be higher than that of larger ones, upon annealing at 500 °C, smaller AgNPs disappear while the larger ones become even larger reaching a mean radius of 67 nm. ITO and AZO samples show remarkable differences with annealing temperatures. At 300 °C annealing, the AgNPs display a normal distribution in a similar way as the other substrates with very high correlation coefficient in the range of $R \geq 0.95$. However, when annealed at 500 °C, we see a substantial increase in the particle size, accompanied with a decrease in the particle density, and a considerable deviation from normal distribution with $R \leq 0.62$.

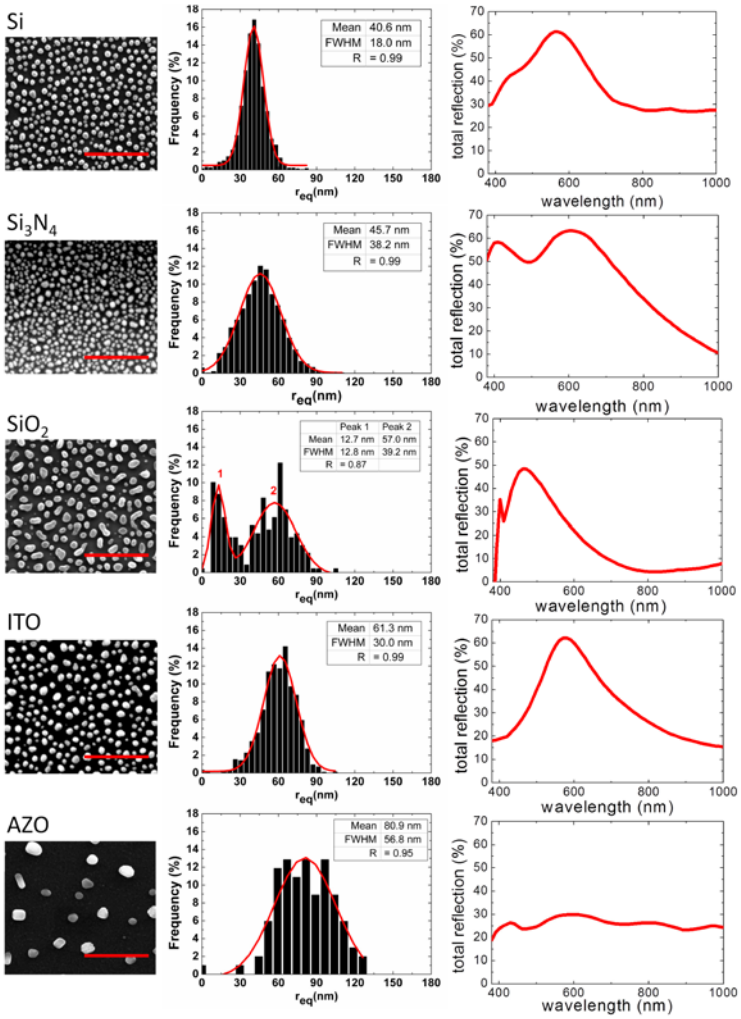

Fig. 2. From left to right: SEM image, equivalent disc radius distribution and total reflection spectrum of AgNPs fabricated at 300 °C on Si, Si_3N_4, SiO_2, ITO and AZO substrates are shown on each raw, respectively. The scale bars in red colour on SEM images correspond to 1 μm distance. The curves in red colour in equivalent radius histograms are Gaussian fits to the data with mean, FWHM and correlation coefficient values (R) as quoted in the inset tables.

Plasmonic peaks are clearly seen in all samples as displayed in the third column of Fig. 2 and Fig. 3. The peak position corresponding to the resonance condition is a strong function of particle size and the local environment. Depending on the substrate and the particle configuration, we observe single and multiple resonance peaks that might be originating from

#188620 - $15.00 USD Received 10 Apr 2013; revised 1 Jul 2013; accepted 3 Jul 2013; published 31 Jul 2013

different sizes, or different type of plasmonic excitations (i.e., dipole and quadrupole). The multipole resonance conditions may also be resulting from the interaction of AgNPs [15]. Besides, from the simple dipole approximations, we know that small AgNPs are more effectively absorbing than larger ones [8]. Moreover, the particle shape [8], and the geometry of the interface between them [12] and the underlying substrate affects the resonance conditions strongly. Hence, it is not a straightforward task to correlate the optical response of an ensemble of dewetting based nanoparticles with a single dominating parameter of the system. Nevertheless, in the following sections, we provide an attempt to describe the effect of substrate on the structural and optical properties in a more detailed way.

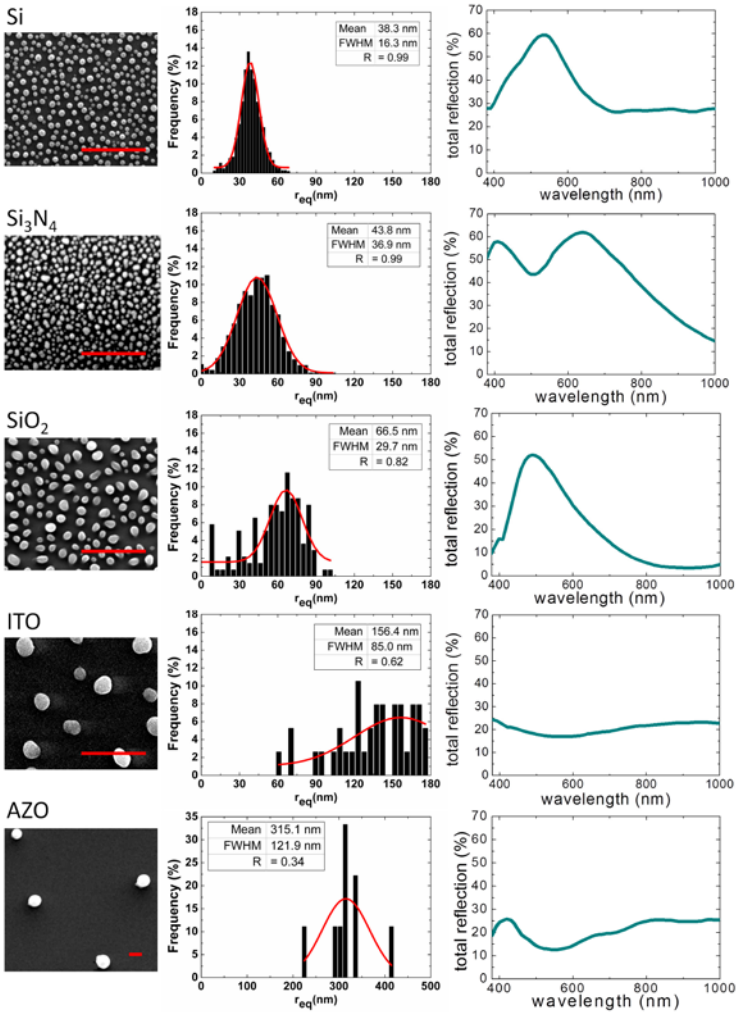

Fig. 3. From left to right: SEM image, equivalent disc radius distribution and total reflection spectrum of AgNPs fabricated at 500 °C on Si, Si_3N_4, SiO_2, ITO and AZO substrates are shown on each raw, respectively. The scale bars in red colour on SEM images correspond to 1 µm distance. The curves in red colour in equivalent disc radius histograms are Gaussian fits to the data with mean, FWHM and correlation coefficient values (R) as quoted in the inset tables.

3.2 Substrate effect on the AgNP formation

Formation of AgNP is driven by the surface energy differences that lead to the decomposition of the thin Ag film into smaller islands. As evidenced from the SiO_2, ITO and AZO samples displayed above, diffusion and merging of small AgNPs with the larger ones also takes place

#188620 - $15.00 USD Received 10 Apr 2013; revised 1 Jul 2013; accepted 3 Jul 2013; published 31 Jul 2013

and result in particle growth on the surface. In the case of AZO we observed as large as 800 nm particle sizes after annealing at 500 °C. The diffusion of metal nanoparticles is a direct function of the local temperature and the stress gradient [16] of the Ag film and nanoparticles formed initially [17–19]. The roughness of the surface might also play a role in the diffusion process. In order to understand the formation kinetics for different substrates, we studied the relation between particle size and the substrate properties. Table 1 summarizes some physical parameters of the substrates used [20–26].

Table 1. Some of the Physical Parameters of the Substrates Used in This Study

	Refractive index (632.8 nm)	Thermal expansion coefficient (/°C)	Thermal diffusivity (m^2s^{-1})	Thermal conductivity ($Wm^{-1}K^{-1}$)	Roughness (nm)
Si	3.88	(2.6×10^{-6}) [20]	$(8. \times 10^{-5})$ [21]	(130) [22]	0.2
Si_3N_4	2.01	(3.3×10^{-6}) [23]	$0.32\text{-}0.84 \times 10^{-4}$	(13-30) [24]	6.4
SiO_2	1.54	(5×10^{-7}) [25]	8.3×10^{-7}	(1.4) [25]	1.6
ITO	1.86	$8.5\text{-}10.2 \times 10^{-6}$	$1.5\text{-}2.2 \times 10^{-6}$	3.2	8.8
AZO	1.99	$4\text{-}5.36 \times 10^{-6}$	$(1.8\text{-}2.4 \times 10^{-6})$ [26]	(5-7) [26]	3.0

In quest for a correlation, we plot the size of AgNPs as a function of substrate thermal conductivity of the substrate as shown in Fig. 4.

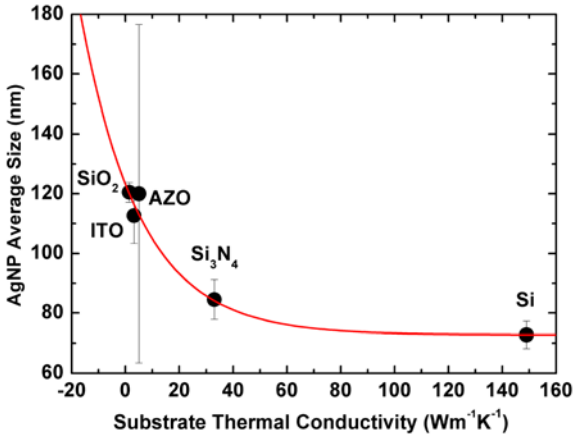

Fig. 4. Average cumulative AgNP size obtained by dewetting at 200 °C, 300 °C, 400 °C and 500 °C vs. substrate thermal conductivity is shown. The red curve is an exponential fit to data with a correlation coefficient of 0.998.

The vertical bars show the standard deviation of the cumulative size spread of AgNPs for each substrate obtained at different annealing temperatures from 200 °C to 500 °C. We see a remarkable correlation between the average AgNP size (black dots) and the substrate thermal conductivity. We obtain larger AgNPs on substrates with lower thermal conductivity. It seems that there is an exponential dependence of the particle size on the thermal conductivity. The red curve is an exponential fit to the average AgNP size of the form: $y = A + Be^{-Cx}$, which yields $A = 72.8$ nm, $B = 50.4$ nm, $C = 0.045$ nm^{-1} with a correlation coefficient of $R = 0.998$. This can be understood and modelled qualitatively by considering the heat transfer between metal film/nanoparticles and the substrates. The heat stored by the metal film and the initially formed islands (or semi islands) is not efficiently transferred to the substrate at least for a certain time interval at the beginning of the annealing process, and thus the steady state temperature of the metal AgNPs is effectively more for substrate with lower thermal conductivity. In order to understand this, let us consider two extreme cases: substrates

#188620 - $15.00 USD Received 10 Apr 2013; revised 1 Jul 2013; accepted 3 Jul 2013; published 31 Jul 2013

with no thermal conductivity and infinite conductivity. In the former case, the radiative heat from the resistive heaters of the furnace will be absorbed and trapped in the metal particles, although some fraction of it will be radiated back to establish a steady state condition. The temperature of the metal film and nanoparticles will then be higher than the substrate if the thermal absorption of the metal is higher than the substrate (which is usually the case). In the latter case, the substrate thermal conductivity is infinite so that the heat transfer takes place easily and a thermal equilibrium between nanoparticles and substrate will quickly be established. In the intermediate cases, which are more like the systems we are studying, the time to reach the thermal equilibrium will depend on the thermal conductivity of the substrate. This will, then, determine the effective temperature of particles on the surface. For substrates with lower thermal conductivity, the temperature of the AgNPs will be higher than those on the substrates with higher conductivity at least for some time interval at the beginning of the annealing process. This will in turn lead to a higher diffusion rate and thus larger AgNPs on the surface.

Another interesting correlation that we observed is between the substrate surface roughness (measured before Ag deposition with AFM) and the FWHM of the AgNP size distribution. We see that the FWHM decreases with the decreasing roughness on the surface. The FWHM appears to have an exponential dependence on the initial substrate surface roughness as seen in Fig. 5.

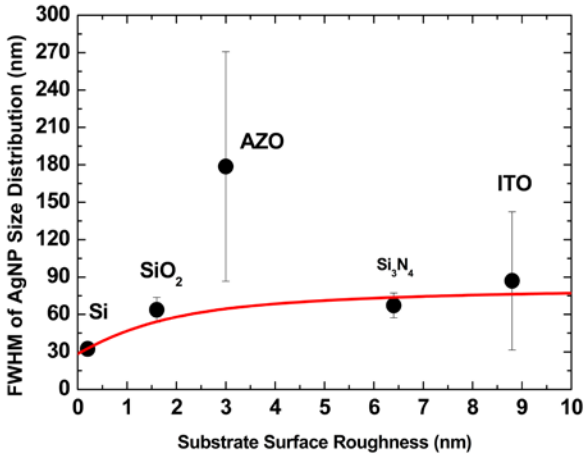

Fig. 5. The FWHM of AgNP size distribution vs. substrate surface roughness measured by AFM is given. The red curve shall serve as a guide to eyes.

As discussed below, rougher surfaces form higher barriers for the particle diffusion leading to more fluctuation in the particle size.

3.3 Optical properties

The positions of the main resonance peak in the total reflection data belonging to selected samples from which a resonance peak could be discerned are displayed in Fig. 6.

#188620 - $15.00 USD Received 10 Apr 2013; revised 1 Jul 2013; accepted 3 Jul 2013; published 31 Jul 2013

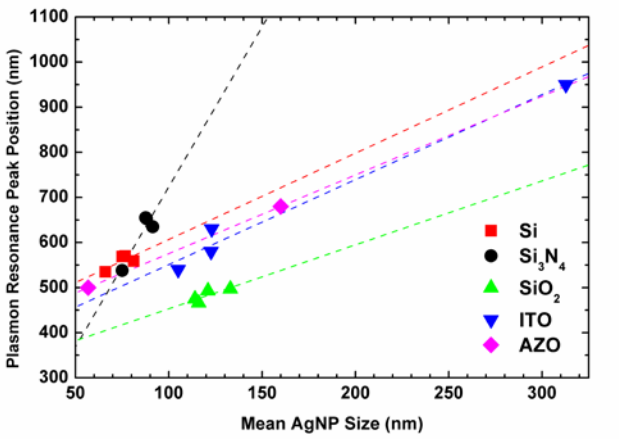

Fig. 6. Resonance peak positions as function of average AgNP size for all substrates are plotted. The dashed lines are linear fits to data with same colours with correlation coefficients ranging 0.58 to 0.98.

Different points of same color correspond to measured mean AgNP size and plasmon resonance peak position obtained at different dewetting temperatures from the same substrate. The dashed lines represent linear fits to the data given in order to serve as guides to the eye. The correlation coefficients range an interval of values from 0.58 (Si) to 0.98 (ITO) exhibiting moderately good to very good correlation to linear dependence for all of the substrate types. In all substrates we observed that the resonance peak shifts to higher wavelengths with increasing average particle size as expected.

4. Discussion and conclusion

With this study we have shown that dewetting based self-organized AgNP decoration of various solar cell related substrates is possible with process temperatures ranging from 200 °C to 500 °C, and we observe a high impact of substrate thermal conductivity on average nanoparticle size and substrate surface roughness on the breadth of nanoparticle size distribution. AgNPs are successfully formed on different surfaces under identical experimental conditions. The formation of AgNPs is found to be strongly affected by the physical properties of the underlying substrate. A strong correlation between the mean AgNP size and the thermal conductivity of the substrate is observed (Fig. 4). The surfaces with lower thermal conductivity yielded larger AgNP sizes. This can be explained by a simple model based on the heat transfer at the metal/substrate interface. The initially formed Ag nanoparticles cannot dissipate the radiative heat that they absorb from their surroundings through the low thermal conducting substrate, causing a local effective temperature increase. Even though the convection is facilitated by N_2 flow during annealing, the local temperature of the nanoparticles under identical conditions will be higher for nanoparticles that are formed on the poorest thermal conductor. This in turn results in larger average AgNPs on such a surface than better thermal conductor surfaces because smaller AgNPs with higher surface diffusivity will eventually merge with more stable larger ones and grow more rapidly. After an identical annealing period as in the case of this study, lower thermal conductor surfaces are expected to have larger average size AgNPs.

Another correlation we observed is in between the roughness of the substrate surface and the FWHM of the size distribution of AgNPs. The flattest substrates exhibit lowest AgNP size dispersion and roughest ones exhibit the largest size dispersion as calculated from the size distribution histograms and FWHM values of the Gaussian fits (Fig. 5). Roughness is likely to pose a surface diffusion barrier for Ag atoms and nanoparticles during the maturation period of the dewetting process. The pits and hills on the path of diffusing Ag atoms, clusters and nanoparticles entrap them for a certain amount of time and eventually hinder the process of merger of smaller nanoparticles with the larger ones. This, in turn, yields in more disperse

#188620 - $15.00 USD Received 10 Apr 2013; revised 1 Jul 2013; accepted 3 Jul 2013; published 31 Jul 2013

sizes of AgNPs around a certain median size, after a finite process time. Rougher the surface larger the expected size dispersion for a given duration and temperature, explaining qualitatively the observed correlation. It should be noted that the surface roughness at the nanoscale can be regarded as an intrinsic property of each chosen substrate because of particular optimized thin film deposition method for each kind of material and therefore it is generally not regarded as a tuning parameter for large area solar cell device fabrication. In our study we did not perform any post deposition process on the substrate surfaces and they are used as grown. In this respect our result shall only serve as a practical guide for readers and shall be used with caution as the surface roughness at the nanoscale may depend strongly on the fabrication process parameters and any possible chemical or physical post processing of the substrate surface.

The reflection data obtained from as grown Ag films on various substrates show rather smoothly varying flat reflection curves around values determined by Fresnel formalism, which are void of any plasmonic resonance peaks due to lack of nanoparticles (data not shown). It is observed that the dewetted Ag film reflects less at regions away from the plasmonic resonance peak wavelength. This result confirms the preferential forward scattering as expected from the AgNP decoration [12]. It should be noted that the reflection from AgNPs exceeds the values of flat Ag film around the resonance wavelength. We woud like to point out that the assessment of overall benefit of decorating solar cells with AgNPs shall, therefore, include an integral differential transmission from the AgNP interface multiplied with the active medium's (Si) absorption for a better judgment for effectiveness in solar cell device performance.

The plasmonic resonance peaks measured from the AgNPs exhibit red shift with increasing average nanoparticle size for all substrate types (Fig. 6). This is in agreement with previously published theoretical and experimental results [11,27]. As the dielectric constants of the substrates given in Table 1 and Fig. 6 suggest, for a given average nanoparticle size the resonance peak position red shifts with the increasing dielectric constant of the substrate. This goes in line with the plasmonic resonance peak position dependence of a single metal nanoparticle embedded in a dielectric medium. Although this simple view qualitatively agrees well with our observations, we believe that the exact configuration of the AgNPs on the substrate surface such as the precise 3D shape, the contact area and contact angle, floating-submersing behaviour of nanoparticles on the surface may play a much more decisive role in the determination of the effective spectral range and strength of the solar cell beneficial optical properties. Furthermore, we observe a distinctly high slope of the linear fit to the Si_3N_4 data when compared to other 4 substrates, suggesting a premature red shift of plasmonic peak position when compared with the data of other 4 substrates. On close inspection of SEM images in Figs. 2 and 3, it is discernible that the average inter-particle distance is smaller in this substrate than all the 4 others. It can be suggested with good confidence that in this substrate the plasmonic interaction between nanoparticles plays a more prominent role than in the others, driving the overall ensemble response of nanoparticles from the resonance peak position of the expected isolated nanoparticle response towards longer wavelengths.

Acknowledgments

A.B. acknowledges the financial support by the European Union FP7-ICT project FOCUS under contract no. 270483 and Middle East Technical University funding under BAP-08-11-2011-129. The authors wish to thank Mr. Sedat Canlı and Mr. Seçkin Öztürk for their support with SEM images. This work has been supported by The Scientific and Technological Research Council of Turkey (TUBITAK) under grant no 109R037 (Rainbow Energy).

#188620 - $15.00 USD Received 10 Apr 2013; revised 1 Jul 2013; accepted 3 Jul 2013; published 31 Jul 2013